Available online at www.sciencedirect.com
ScienceDirect
Journal of Hazardous Materials 155 (2008) 312–319
Journal of Hazardous Materials
www.elsevier.com/locate/jhazmat

Photocatalytic degradation of Orange G on nitrogen-doped TiO_2 catalysts under visible light and sunlight irradiation

Jianhui Sun [a,*], Liping Qiao [a,b], Shengpeng Sun [a], Guoliang Wang [a]

[a] *Henan Key Laboratory for Environmental Pollution Control, Henan Normal University, College of Chemistry and Environmental Science, No. 46, Jianshe Road, Xinxiang, Henan Province 453007, PR China*
[b] *Department of Environmental Science and Engineering, Fudan University, No. 220, Handan Road, Shanghai 200433, PR China*

Received 23 December 2006; received in revised form 16 November 2007; accepted 20 November 2007
Available online 23 November 2007

Abstract

In this paper, the degradation of an azo dye Orange G (OG) on nitrogen-doped TiO_2 photocatalysts has been investigated under visible light and sunlight irradiation. Under visible light irradiation, the doped TiO_2 nanocatalysts demonstrated higher activity than the commercial Dugussa P25 TiO_2, allowing more efficient utilization of solar light, while under sunlight, P25 showed higher photocatalytic activity. According to the X-ray diffraction (XRD), X-ray photoelectron spectroscopy (XPS) and UV–vis spectra analyses, it was found that both the nanosized anatase structure and the appearance of new absorption band in the visible region caused by nitrogen doping were responsible for the significant enhancement of OG degradation under visible light. In addition, the photosensitized oxidation mechanism originated from OG itself was also considered contributing to the higher visible-light-induced degradation efficiency. The effect of the initial pH of the solution and the dosage of hydrogen peroxide under different light sources was also investigated. Under visible light and sunlight, the optimal solution pH was both 2.0, while the optimal dosage of H_2O_2 was 5.0 and 15.0 mmol/l, respectively.

Keywords: Photocatalytic degradation; Photosensitized oxidation; Visible light; Sunlight; Nitrogen-doped TiO_2

1. Introduction

Azo dyes, which are characterized by the presence of one or more azo bonds (–N=N–), are among the most notorious widespread environmental pollutants associated with textile, cosmetic, food colorants, printing, and pharmaceutical industries. Because of their non-degradability, toxicity, potential mutagenicity and carcinogenicity, wastewaters originating from these dyes production or application industries pose a major threat to the surrounding ecosystems and human beings' health [1–3]. Environmental concerns and the need of meeting the stringent international standards for rejecting wastewaters has made the development of novel and cost-effective processes for the purification of azo dyes effluents an issue of major technological importance.

Advanced oxidation processes (AOPs) have been proposed and widely investigated for the degradation of recalcitrant materials in wastewaters since the 1990s. Among them, TiO_2 mediated heterogeneous photocatalysis has been showed to be potentially advantageous as it may proceed at ambient conditions and lead to the complete mineralization of many organic pollutants to harmless products of CO_2, H_2O and mineral acids [4,5]. However, because of the relatively large band-gap, TiO_2 is activated only by ultraviolet light with wavelengths shorter than 387 nm, which constitutes only about 3–5% of the solar spectra. Practically, this factor strongly limits the use of solar spectra as a light source. On the other hand, the conversion efficiency of generating UV light from electricity in a photocatalytic system is usually less than 20% [6], and the utilization efficiency of these electricity-generated light photons to decompose the pollutants is also no more than 5% [7,8]. In other words, less than 1% electrical energy is virtually utilized in an UV-photocatalytic system. Obviously, UV light source should be avoided from energy saving point of view, and the most desired light source lies ultimately on solar energy. From this viewpoint, development of new approaches to sensitize TiO_2 catalysts efficiently with the much larger visible light would be of great significance for practical and widespread use.

* Corresponding author. Tel.: +86 373 3325971; fax: +86 373 3326336.
E-mail address: sunjh@henannu.edu.cn (J. Sun).

0304-3894/$ – see front matter © 2007 Elsevier B.V. All rights reserved.
doi:10.1016/j.jhazmat.2007.11.062

Nowadays, the methods for achieving the visible-light-driven photocatalysis are widely investigated [5,9]. One effective approach is based on modification of TiO_2 by various metal ions [10,11] or non-metallic species such as nitrogen, carbon, sulfur, boron, phosphor, fluorine, iodine [12–19], which can move the spectra of TiO_2 into the main part of solar spectra ($\lambda > 380$ nm). Among these, the simplest and most feasible approach seems to be nitrogen doping [12], that is, doping nitrogen atoms into substitutional sites in the crystal structure of TiO_2 (e.g., $TiO_{2-x}N_x$) by calcination in ammonia atmosphere or by a wet chemical route [20–25]. Another approach lies on photosensitization of TiO_2 by a variety of colored organic compounds [9,26–28], which can be excited to the singlet or triplet states by visible light and then inject electrons into the conduction band of TiO_2. On condition that colored pollutants such as azo dyes were being degraded, this photosensitized oxidation process being initiated by the-dye-itself would be much fascinating.

Photocatalytic degradation of Orange G (OG) has been reported in several studies [29–32], and many investigations focused widely on the UV-illuminated TiO_2 processes [33–39]. Nagaveni et al. [40] conducted the degradation of OG using combustion-synthesized nano-TiO_2 under solar light, and found that the initial degradation rates were 1.6 times higher than that using Degussa P25 TiO_2. They attributed the enhanced photocatalytic activity to the crystallinity, nanosize, large amount of surface hydroxyl species and reduced band-gap. Still no major effort has been made to study OG degradation driving by visible light.

In the present investigation, we have undertaken degradation of OG on nitrogen-doped TiO_2 (N-doped TiO_2) photocatalysts under visible light and sunlight irradiation. The X-ray diffraction (XRD), X-ray photoelectron spectroscopy (XPS) and UV–vis spectra were all used to characterize the catalysts and aimed at finding the origin of the photocatalytic activity under different light sources. The effect of the variables such as the initial solution pH and the dosage of hydrogen peroxide were also investigated.

2. Experimental

2.1. Reagents and photocatalysts

Azo dye OG, a reagent in molecular biology, $C_{16}H_{10}N_2Na_2OS_2$ (7-hydroxy-8-phenlyazo-1, 3-naphthalenedisulfonic acid disodium salt), was obtained from Shanghai Reagent Co. (Shanghai, China) and was used without further purification. The molecular structure of OG and its UV–vis absorption spectra are presented in Fig. 1. Tetrabutyl titanate ($Ti(OBu)_4$, 99%, w/w), ammonia (28–30%, w/w), hydrogen peroxide (H_2O_2), nitric acid and sodium hydroxide were all of analytical grade and obtained from Tianjin Kermal Chemical Reagents Co. (Tianjin, China). The commercial Degussa P25 TiO_2 was purchased from Germany Degussa Co. (Germany).

The N-doped TiO_2 photocatalysts were prepared by calcination of the hydrolysis product of $Ti(OBu)_4$ with ammonia as precipitator. Typically at room temperature, 20 ml of $Ti(OBu)_4$ solution was hydrolyzed by dropwise addition of 10 ml aqueous ammonia with a rate of 1 ml/min under vigorous stirring. After continuously stirring for 30 min, the mixture obtained was transferred to a culture dish and dried at 373 K for 2 h in an oven. Finally, the yellowish N-doped catalysts particles were obtained through calcinating the white powders in a muffle furnace at 723 K for 2 h. For comparison, we also obtained the non-doped TiO_2 by the hydrolysis of $Ti(OBu)_4$ with pure water using the same procedure as done for doped samples.

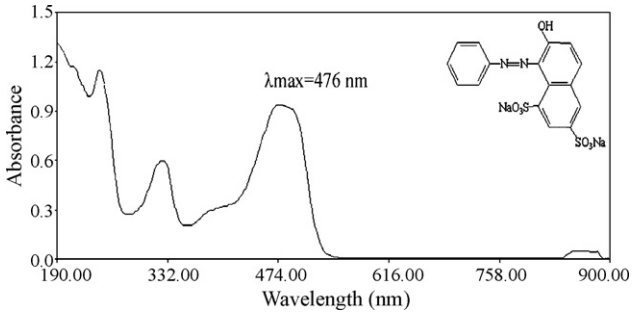

Fig. 1. Molecular structure of OG and its UV–vis absorption spectra.

The obtained photocatalysts were ground in agate mortar before further analysis or use. All experiments were carried out with use of deionized water.

2.2. Catalyst characterization

The crystal structures of the catalysts were analyzed by X-ray powder diffraction. The XRD analysis was carried out on a Bruker-D8-AXS diffractometer system (Bruker Co., Germany) equipped with a Cu Kα radiation ($\lambda = 0.15406$ nm) and a graphite monochromatic operation at 45 kV and 40 mA. The patterns were obtained at a scan rate of 0.020°/0.4 s. The average crystal size was estimated by the Scherrer equation using the full width at half maximum (FWHM) data after correcting the instrumental broadening. The light absorption properties of the catalysts were studied by UV–vis spectroscopy. The UV–vis spectra were recorded on a Jasco V-550 spectrophotometer equipped with an integrating sphere and using $BaSO_4$ as reference. The elements composition of the catalysts and their corresponding chemical states were investigated by XPS. The XPS spectra were acquired with an Axis Ultra-Kratos spectrometer using Al Kα radiation as X-ray source, and all the binding energies were calibrated to the C1s peak at 284.8 eV of the surface adventitious carbon.

2.3. Experimental setup and procedures

For experiments under visible light, the photoreactor is shown in Fig. 2. Light was provided by a 500 W Xenon-arc lamp (Shanghai Jiguang Co., Shanghai), which emitted almost exclusively light at $\lambda > 400$ nm. The lamp was placed in the inner tube, which was surrounded by the second tube connected to a water bath to maintain the solution at 298 ± 1 K. The third tube was filled with 2 mol/l $NaNO_2$ solution to avoid ultraviolet irradiation. The photocatalytic reactions took place in the outer

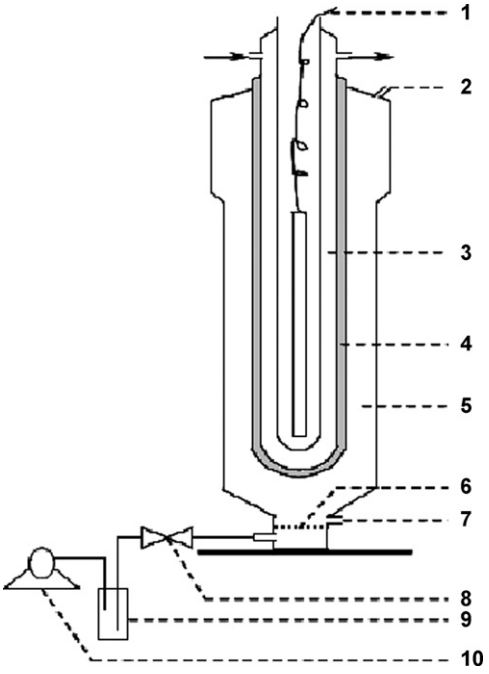

Fig. 2. Photoreactor employed under visible light irradiation: (1) xenon lamp; (2) air outlet and reactant inlet; (3) glass cooling jacket with water; (4) interlayer with $NaNO_2$ solution; (5) outer vessel for reaction mixture; (6) aeration board; (7) discharge outlet; (8) gas flowmeter; (9) buffer bottle and (10) air compressor.

vessel. And the reaction solution was stirred by the bubble of atmosphere air with a flow rate of 0.2 m^3/h through the aeration board at the bottom.

The sunlight experiments were carried out in 1500 ml beakers between 12:00 and 14:00 during the months of November (winter season) at latitude 35°19′ North and longitude 113°54′ East (Xinxiang, Henan province in China). The solution was stirred with magnetic stirrer.

Initial reaction mixture was 1000 ml of 25 mg/l OG solution containing 1.00 g/l catalysts, with different initial pH values and H_2O_2 dosages. Before irradiation, the solution was first ultrasonicated for 15 min, and then stirred for 45 min in the dark to ensure adsorption equilibrium between the catalysts and the solution. Then irradiating and timing, samples were taken at given intervals, centrifuged (3500 rpm for 10 min) and subsequently filtered through a 0.45 μm membrane filter to remove the catalysts.

The concentration of the remaining dye in the solution was determined by measuring the absorbance intensity at 476 nm (Lambda-17 spectrophotometer, PerkinElmer) and with the use of calibration curves. The degradation efficiency of OG was defined as follows (Eq. (1)):

$$\text{Degradation efficiency}(\%) = \frac{C_0 - C_t}{C_0} \times 100\% \quad (1)$$

where C_0 is the concentration of OG after adsorption equilibrium in the dark ($t = 0$), and C_t is the concentration of OG at reaction time t (min).

All these experiments were conducted in triplicates and the results were showed at the mean values.

3. Results and discussion

3.1. Photocatalyst characterization

3.1.1. Structure analysis

Fig. 3 shows the XRD patterns for the N-doped and the non-doped catalysts. Only the diffraction peaks identified as an anatase structure were observed without any contamination from other phases such as rutile or brookite structure. By applying the Scherrer equation, the average particle sizes were estimated to be 14.0 and 15.3 nm for the doped and non-doped TiO_2, respectively. It is notable that, even the doped samples exhibit typical structure of TiO_2 crystal without any detectable dopant related peaks. This may be caused by the lower concentration of the doped species, and moreover, the limited dopants may have moved into either the interstitial positions or the substitutional sites of the TiO_2 crystal structure [41].

3.1.2. X-ray photoelectron spectroscopy

XPS analysis was used to determine the chemical states and concentration of each element possibly existing in the samples. Fig. 4 shows the XPS survey spectra of the doped and the non-doped TiO_2. Elements of Ti, O, N and C were confirmed to exist in the doped nanoparticles by the four peaks at binding energies of 458.8, 530.1, 398.7 and 284.8 eV, which were related to Ti2p, O1s, N1s, and C1s, respectively. And the mass concentration of these four elements Ti, O, N and C was 34.92, 57.08, 1.76, 6.24%, respectively. Whereas, in the non-doped samples, nitrogen was completely absent.

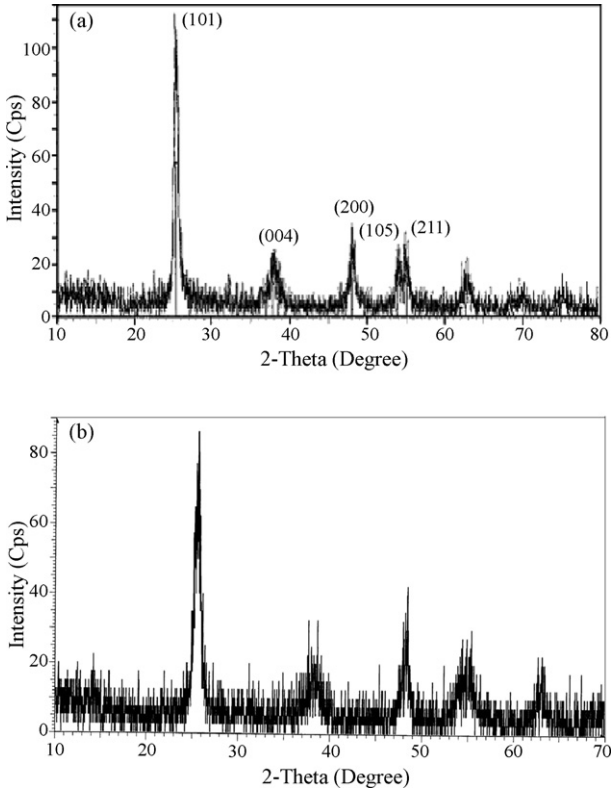

Fig. 3. XRD patterns of (a) the N-doped TiO_2, and (b) the non-doped TiO_2.

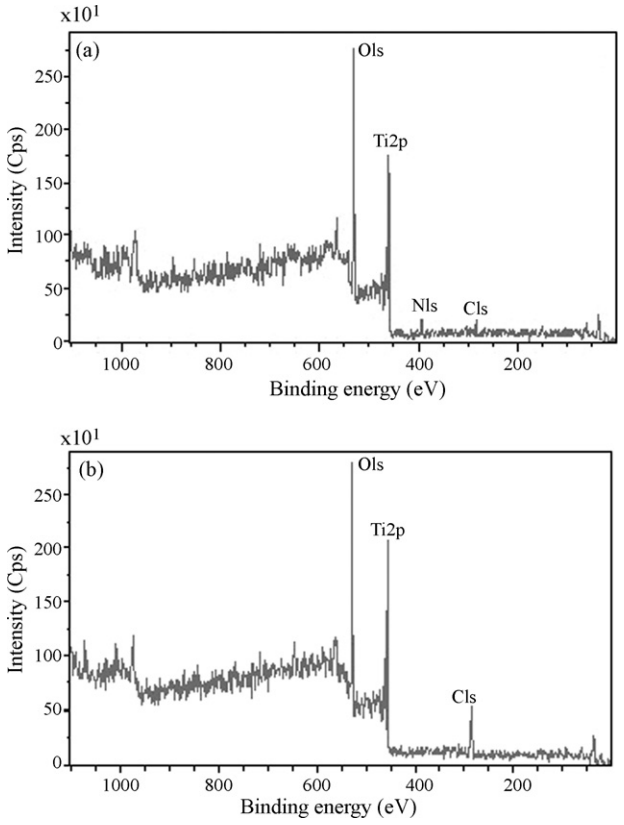

Fig. 4. XPS survey spectra of (a) the N-doped TiO_2, and (b) the non-doped TiO_2.

To investigate the chemical states of N atoms in the doped TiO_2, we measured N1s core levels with XPS spectra (Fig. 5). Two peak structures at binding energies of 400.2 and 398.7 eV were observed. The first peak at binding energy of 400.2 eV was assigned as the molecular chemisorbed γ-N_2 [12,42]. The latter peak was considered arising from Ti–N bonds in TiO_2 [12,22]. By comparing with the typical binding energy of 396.9 eV in TiN [43], the latter peak was 1.8 eV higher and, therefore, was attributed to the 1s electron binding energy of the N atom in the environment of O–Ti–N. This shift of binding energy might be explained by the fact that, when N atom substituted for O

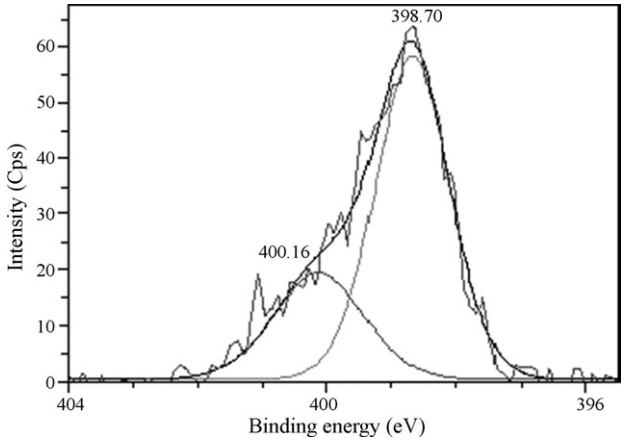

Fig. 5. N1s XPS spectra of the N-doped TiO_2.

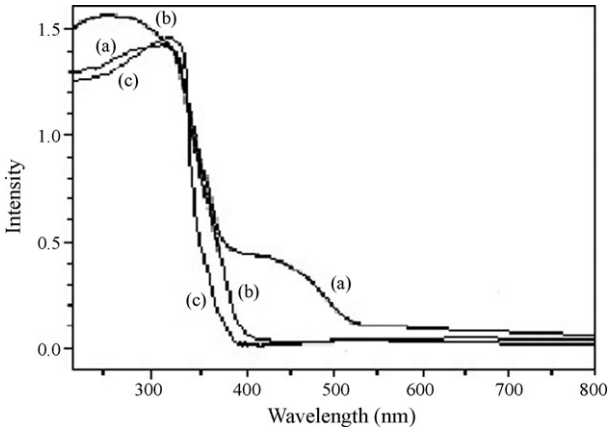

Fig. 6. UV–vis absorption spectra of (a) the N-doped TiO_2, (b) Degussa P25 TiO_2, and (c) the non-doped TiO_2.

atom in the initial O–Ti–O structure, the electron density around N was reduced compared to that in the N–Ti–N structure of TiN crystal, because of the much higher electronegativity of O atom.

3.1.3. UV–vis diffuse reflectance spectroscopy

Optical absorption spectra of the N-doped, non-doped and P25 TiO_2 are shown in Fig. 6. The absorption measurements of the N-doped TiO_2 powders showed a new absorption band in the visible range of 400–550 nm, whereas the non-doped TiO_2 and P25 TiO_2 only exhibited the fundamental absorption edge of TiO_2, which is located in the UV region at about 387 nm. By comparing the spectra of the N-doped TiO_2 with the non-doped TiO_2, it was found from the case of non-doped TiO_2 that, C atoms appeared not to affect the optical absorption properties of TiO_2. Thus, we attribute this new absorption band to the doped nitrogen. Furthermore, the color of the doped powders was vivid yellow while the non-doped and P25 powders were both white. And in general, the color of a solid is determined by the position of its absorption edge; a shift of this absorption edge towards a higher wavelength can result in absorption in the visible range of spectra. For the colored N-doped samples, this shift could be ascribed to the doping of N atoms [44]. This also strongly supported the conclusion that the appearance of a new absorption band in the visible region in the doped powders was originated from the nitrogen doping.

3.2. Degradation of OG

To explore the photo-degradability of OG on the N-doped TiO_2 catalysts under visible light and sunlight irradiation, a series of experiments were performed according to the similar procedure. P25 TiO_2, which was always used as standard materials to evaluate the activity of TiO_2 nanoparticles synthesized through other routines, has been reported being capable of photosensitized oxidation of azo dyes under visible light [26–28]. So herein, P25 TiO_2 was used as referent. In addition, considering the similar procedure in synthesis and the slight differences in compositions, the photocatalytic behavior of non-doped TiO_2 was also measured.

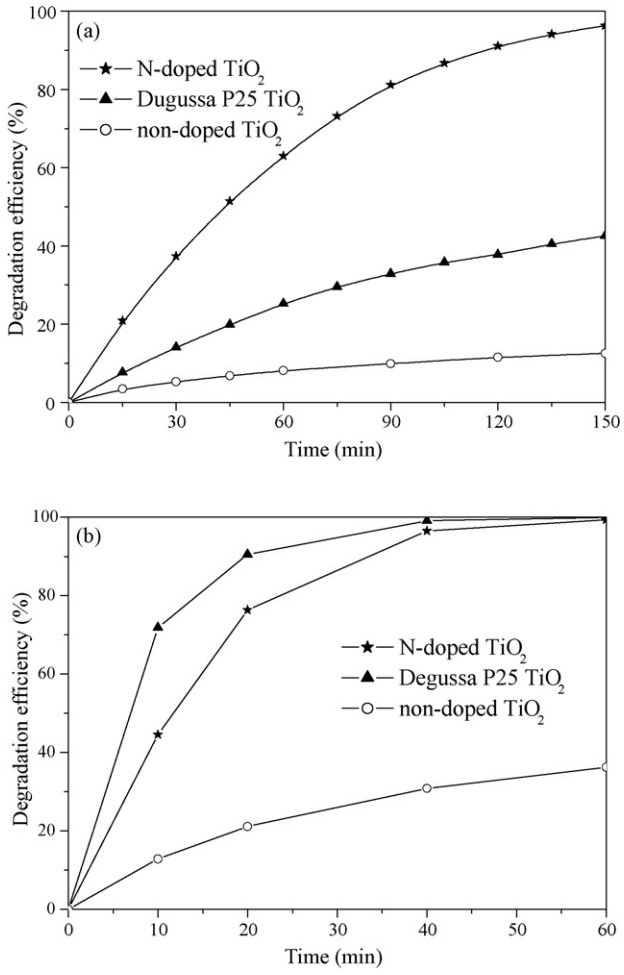

Fig. 7. Photodegradation of OG under (a) visible light (pH = 2.0, $[H_2O_2]$ = 5.0 mmol/l) and (b) sunlight irradiation (pH = 2.0, $[H_2O_2]$ = 15.0 mmol/l).

3.2.1. Visible-light-induced degradation of OG

Fig. 7(a) shows the photodegradation of OG on different catalysts under visible light irradiation. Obviously, the N-doped TiO_2 exhibited the highest degradation efficiency with 96.29% of OG being degraded in 150 min, while P25 showed 42.55% conversion and the non-doped TiO_2 showed less than 13.0% conversion in the same test period. Compared with P25, which is considered as excellent and standard photocatalysts, the enhancement in OG degradation under visible light using the N-doped TiO_2 is certainly significant. Such results can be explained from several aspects.

Firstly, it was demonstrated from the relatively lower degradation efficiency with the non-doped TiO_2 that C atoms existing in it or even in the doped TiO_2 would be not the origin of visible activity. This conclusion coincides with the zero optical absorption properties of the non-doped catalysts in the visible range as shown in Fig. 6. And the new absorption band observed in the visible range as discussed in Section 3.1.3 might just be the reason for the great improvement in OG degradation for the N-doped TiO_2. It is just nitrogen doping that lowered the bandgap energy of the N-doped TiO_2 and lead to the red shift of catalysts' absorption band. Thus, the doped catalysts could absorb visible light and be activated to generate pairs of electrons–holes (h^+–e^-), which would participate directly in the photocatalytic reactions.

Secondly, the smaller particle size of the doped TiO_2, which could lead to the increase of active sites on the TiO_2 surface, provided another powerful explanation.

In addition, certain degradation efficiency achieved with P25 and the non-doped TiO_2 demonstrated another reason called photosensitized oxidation mechanism. It suggests that under visible light, the adsorbed dye is excited to appropriate singlet ($^1Dye^*$) or triplet ($^3Dye^*$) states, subsequently the electron is injected from the excited dye molecule onto the conduction band of the TiO_2 particles, whereas the dye is converted to the cation dye radicals ($Dye^{\bullet+}$) that undergoes degradation to yield products as follows (Eqs. (2)–(5)) [5,26–28]:

$$Dye + h\nu(\text{visible light}) \rightarrow {}^1Dye^* + {}^3Dye^* \quad (2)$$

$$^1Dye^* \text{or} ^3Dye^* + TiO_2 \rightarrow Dye^{\bullet+} + TiO_2(e_{CB}{}^-) \quad (3)$$

$$TiO_2(e_{CB}{}^-) + O_2 \rightarrow O_2{}^{\bullet-} + TiO_2 \quad (4)$$

$$Dye^{\bullet+} \rightarrow \text{degradation products} \quad (5)$$

where the cation dye radicals can readily react with hydroxyl ions (OH^-) undergoing oxidation with $HO^\bullet$ species or interact efficiently with $O_2{}^{\bullet-}$, $HO_2{}^\bullet$ or $HO^\bullet$ species to generate intermediates that ultimately lead to CO_2.

3.2.2. Solar light induced degradation of OG

Fig. 7(b) illustrates the photodegradation of OG on different catalysts under sunlight irradiation. It was observed that under sunlight, the degradation efficiency of OG with P25 was higher than that with the N-doped TiO_2, whereas it was exactly the opposite being observed under visible light. And the non-doped TiO_2 also induced 36.24% of OG degradation in 60 min.

Compared with the light sources, the most essential distinctness of them is the existence of UV light in the sunlight. Therefore, we could contribute the relatively higher photocatalytic efficiency of OG on P25 to the UV light existing in solar light. And this conclusion could be further confirmed by the stronger optical absorption of P25 in UV region than the doped TiO_2, which was observed in Fig. 6. In addition, the high dispersibility and the well-developed crystallinity of P25 TiO_2 containing anatase and rutile phases in a ratio of 80:20, which meant a low density of recombination centers, were probably another reason [45].

Thus, the imperfections of such synthesized catalysts should be pointed out to be that, although the N-doped TiO_2 can be excited by both visible and UV light and exhibited significant degradation efficiency under visible light, its degradation efficiency of OG was still not comparable with P25 under sunlight irradiation.

3.3. Effect of operational parameters under different light sources

3.3.1. Effect of solution pH

The wastewater from textile industries usually has a wide range of pH values. Generally, the pH of the solution is an

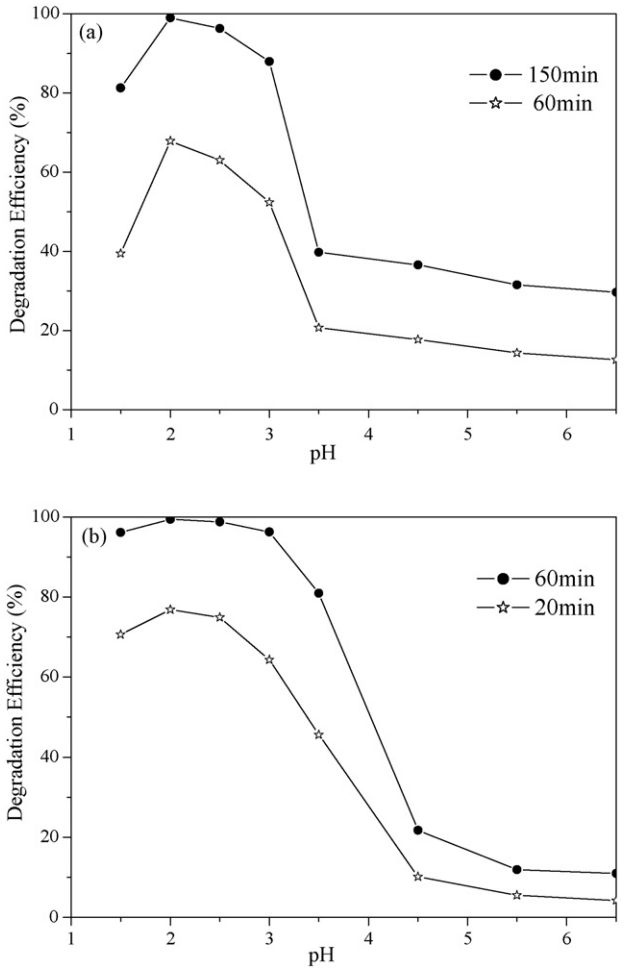

Fig. 8. Effect of pH on degradation of OG with the N-doped TiO_2 under (a) visible light ($[H_2O_2] = 5.0$ mmol/l) and (b) sunlight irradiation ($[H_2O_2] = 15.0$ mmol/l).

important parameter in the photocatalytic processes, since it not only plays an important role in the characteristics of textile wastewater, but also determines the surface charge properties of TiO_2, the size of aggregates formed, the charge of dye molecules, adsorption of dyes onto TiO_2 surface and the concentration of hydroxyl radicals. Hence, the photodegradation of OG on the N-doped TiO_2 was studied in pH range from 1.5 to 6.5. Fig. 8 demonstrates the effect of pH on the degradation of OG under different light sources. It was found that decrease of solution pH from 6.5 to 2.0 increased the degradation efficiency of OG from 31.67 to 98.98% at 150 min under visible light and from 8.00 to 99.37% at 60 min under sunlight. Further decrease of solution pH from 2.0 to 1.5 would decrease the degradation efficiency under both light sources. Thus, the pH of solution significantly influences the degradation of OG and 2.0 was the optimal solution pH under both the visible light and sunlight.

According to the point of zero charge (Pzc), the surface charge property of TiO_2 changes with the change of solution pH. The pH_{Pzc} for TiO_2 is widely reported at 6.25–6.90. Thus, TiO_2 surface is presumably positively charged in acidic solution ($pH < pH_{Pzc}$) and negatively charged in alkaline solution ($pH > pH_{Pzc}$) as given in Eqs. (6) and (7) [46,47]:

$$pH < pH_{Pzc}: TiOH + H^+ \rightleftharpoons TiOH_2^+ \quad (6)$$

$$pH > pH_{Pzc}: TiOH + OH^- \rightleftharpoons TiO^- + H_2O \quad (7)$$

The OG dye in solution is negatively charged as the sulphonated group existing in its structure is hydrolyzed. Due to the electrostatic attraction, the acidic solution favors adsorption of OG dye onto TiO_2 surface, and the degradation efficiency of OG increases accordingly.

However, further lowering the solution pH (below 2.0) creates the agglomeration of TiO_2 particles, which will reduce the surface area available for dye adsorption and photon absorption [48]. Moreover, at low pH the concentration of H^+ is in excess, and the H^+ ions interact with the azo linkage (–N=N–), which is particularly susceptible to be electrophilic attacked by hydroxyl radical, decreasing the electron densities at azo group [49]. Consequently, the reactivity of hydroxyl radical by electrophilic mechanism decreases.

3.3.2. *Effect of dosage of H_2O_2*

One practical problem in using TiO_2 as photocatalysts is the undesired electron–hole recombination, which in the absence of proper electron acceptor or donor, is extremely efficient and thus represents the major energy-wasting step thereby limiting the achievable quantum yield. One strategy to inhibit electron–hole recombination is to add irreversible electron acceptors to the reaction system, and usually H_2O_2 was used for this purpose. The effect of H_2O_2 dosage on photodegradation of OG on the N-doped TiO_2 under different light sources was investigated. The results are shown in Fig. 9. The results indicated that there was an optimal dosage of H_2O_2, at which the degradation efficiency of OG on the N-doped TiO_2 attained the height. Below the optimal dosage, the enhancement of degradation by addition of H_2O_2 could be attributed to the increase of reactive hydroxyl radical concentration according to the following Eqs. (8) and (9) [50]:

$$TiO_2(e_{CB}^-) + H_2O_2 \rightarrow TiO_2 + {}^\bullet OH + OH^- \quad (8)$$

$$O_2^{\bullet -} + H_2O_2 \rightarrow OH^- + {}^\bullet OH + O_2 \quad (9)$$

But when H_2O_2 presented at higher dosage, the degradation efficiency of OG decreased. This was because the very reactive $^\bullet OH$ radicals and valence band holes could be consumed by H_2O_2 itself as given in Eqs. (10)–(12) [5,51]. At the same time, radical–radical recombination as a competitive reaction must be taken into account, as described in Eq. (13) [52].

$$^\bullet OH + H_2O_2 \rightarrow HO_2^\bullet + H_2O \quad (10)$$

$$^\bullet OH + HO_2^\bullet \rightarrow O_2 + H_2O \quad (11)$$

$$TiO_2(h_{VB}^+) + H_2O_2 \rightarrow TiO_2 + O_2 + 2H^+ \quad (12)$$

$$HO^\bullet + HO^\bullet \rightarrow H_2O_2 \quad (13)$$

As both $^\bullet OH$ and h_{VB}^+ are strong oxidants for organic pollutants, the photocatalytic degradation of OG will be inhibited in the condition of excess of H_2O_2. Furthermore, H_2O_2 can

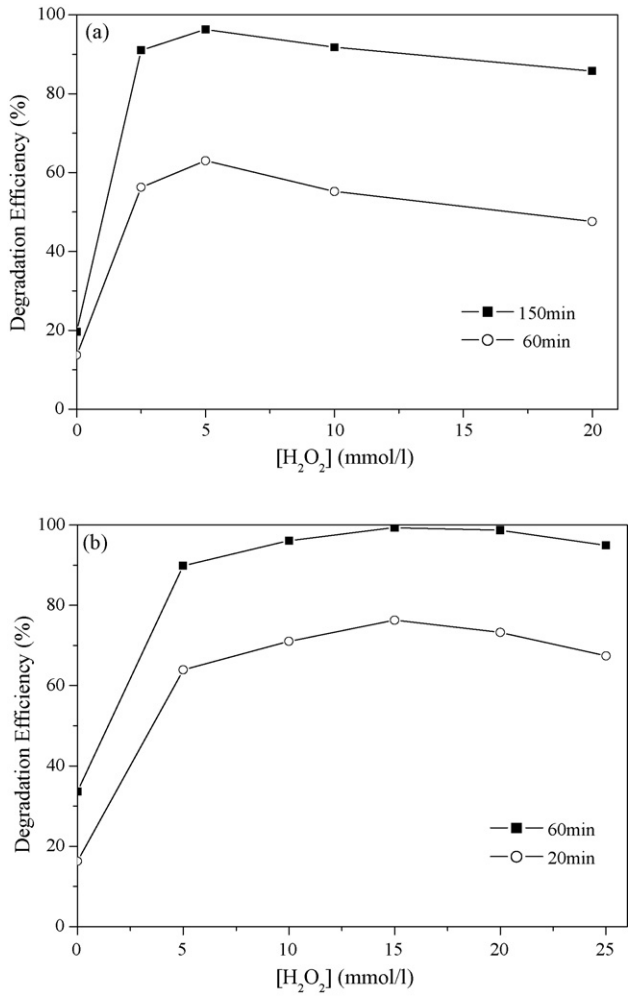

Fig. 9. Effect of dosage of H_2O_2 on degradation of OG with the N-doped TiO_2 under (a) visible light (pH = 2.0) and (b) sunlight irradiation (pH = 2.0).

be adsorbed onto TiO_2 particles to modify their surfaces and subsequently decrease its catalytic activity [53].

Compared with the optimal dosage of H_2O_2, which is 5.0 mmol/l, 15.0 mmol/l under visible light and sunlight, respectively, it is found that they are not identical with each other as the optimal solution pH exhibited. This may result from the difference in wavelength and intensity of the two light sources. What's more, the UV light existing in the sunlight has higher energy intensity to excite the catalysts and will generate more electron–hole pairs, which may need different dosage of electron acceptors, such as H_2O_2. Thus, the optimal dosage of H_2O_2 may vary with the change of light sources, and in order to keep higher photodegradation efficiency, it is necessary to choose the optimal dosage of H_2O_2 under different light sources.

4. Conclusions

Treatment of simulated wastewater containing azo dye OG using photocatalytic process has been taken into consideration in the present study. The N-doped TiO_2, prepared by the calcination of the hydrolysis product of tetrabutyl titanate with ammonia as precipitator was used as catalysts, and artificial visible light and natural sunlight were used as light sources. The XRD analysis showed that the catalysts were nanosized anatase structure. The XPS and UV–vis spectra indicated that the nitrogen doping caused the new absorption band appeared in the visible region. The degradation efficiency of OG with the N-doped TiO_2 was much higher than that with P25 under visible light irradiation. It is considered that not only the new absorption band in visible range originated from the nitrogen doping and the smaller particle size, but also the photosensitized oxidation mechanism originated from the azo dyes themselves contributed to the higher visible-light-activity. In contrast, P25 exhibited higher photocatalytic activity under sunlight irradiation. Based on the experimental results presented above, it has been found that the initial solution pH and the addition of H_2O_2 both significantly influenced the degradation efficiency of OG. And the optimal solution pH was both 2.0 under the two light sources, while the optimal dosage of H_2O_2 was 5.0 and 15.0 mmol/l under visible light and sunlight irradiation, respectively. Based on these results, it will be of significance to explore the operational parameters under different light sources.

Acknowledgements

The authors wish to gratefully acknowledge the support from the Key Science & Technology Research Project of Henan province, People's Republic of China (Grant No. 0523032200).

References

[1] K.-T. Chung, G.E. Fulk, A.W. Andrews, Mutagenicity testing of some commonly used dyes, Appl. Environ. Microbiol. 42 (1981) 641–648.
[2] B.N. Ames, J. McCann, E. Yamasaki, Methods for detecting carcinogens and mutagens with the Salmonella/mammalian microsome mutagenicity test, Mutat. Res. 31 (1975) 347–364.
[3] H.M. Pinheiro, E. Touraud, O. Thomas, Aromatic amines from azo dye reduction: status review with emphasis on direct UV spectrophotometric detection in textile industry wastewaters, Dyes Pigment. 61 (2004) 121–139.
[4] O. Legrini, E. Oliveros, A.M. Braun, Photochemical processes for water treatment, Chem. Rev. 93 (1993) 671–698.
[5] I.K. Konstantinou, T.A. Albanis, TiO_2-assisted photocatalytic degradation of azo dyes in aqueous solution: kinetic and mechanistic investigations: a review, Appl. Catal. B-Environ. 49 (2004) 1–14.
[6] H. Taoda, Book on Photocatalysis, Nikan kougyou Tokyo, 2002.
[7] A. Mills, S.L. Hunte, An overview of semiconductor photocatalysis, J. Photochem. Photobiol. A-Chem. 108 (1997) 1–35.
[8] W. Choi, A. Termin, M.R. Hoffmann, The role of metal ion dopants in quantum-sized TiO_2: correlation between photoreactivity and charge carrier recombination dynamics, J. Phys. Chem. B 98 (1994) 13669–13679.
[9] D. Chatterjee, S. Dasgupta, Visible light induced photocatalytic degradation of organic pollutants, J. Photochem. Photobiol. C-Photochem. Rev. 6 (2005) 186–205.
[10] S. Kim, S.-J. Hwang, W. Choi, Visible light active platinum-ion-doped TiO_2 photocatalyst, J. Phys. Chem. B 109 (2005) 24260–24267.
[11] J. Zhou, M. Takeuchi, X.S. Zhao, A.K. Ray, M. Anpo, Photocatalytic decomposition of formic acid under visible light irradiation over V-ion-implanted TiO_2 thin film photocatalysts prepared on quartz substrate by ionized cluster beam (ICB) deposition method, Catal. Lett. 106 (2006) 67–70.
[12] R. Asahi, T. Morikawa, T. Ohwaki, K. Aoki, Y. Taga, Visible-light photocatalysis in nitrogen-doped titanium oxides, Science 293 (2001) 269–271.

[13] H. Wang, J.P. Lewis, Second-generation photocatalytic materials anion-doped TiO_2, J. Phys. Condense Matter. 18 (2006) 421–434.
[14] S. Yin, K. Ihara, Y. Aita, M. Komatsu, T. Sato, Visible-light induced photocatalytic activity of $TiO_{2-x}A_y$ (A = N, S) prepared by precipitation route, J. Photochem. Photobiol. A-Chem. 179 (2006) 105–114.
[15] T. Ohno, T. Tsubota, M. Toyofuku, R. Inaba, Photocatalytic activity of a TiO_2 photocatalyst doped with C^{4+} and S^{4+} ions having a rutile phase under visible light, Catal. Lett. 98 (2004) 255–258.
[16] W. Ren, Z. Ai, F. Jia, L. Zhang, X. Fan, Z. Zou, Low temperature preparation and visible light photocatalytic activity of mesoporous carbon-doped crystalline TiO_2, Appl. Catal. B-Environ. 69 (2007) 138–144.
[17] L. Lin, W. Lin, J.L. Xie, Y.X. Zhu, B.Y. Zhao, Y.C. Xie, Photocatalytic properties of phosphor-doped titania nanoparticles, Appl. Catal. B-Environ. 75 (2007) 52–58.
[18] X. Hong, Z. Wang, W. Cai, F. Lu, J. Zhang, Y. Yang, N. Ma, Y. Liu, Visible-light-activated nanoparticle photocatalyst of iodine-doped titanium dioxide, Chem. Mater. 17 (2005) 1548–1552.
[19] D. Li, H. Haneda, N.K. Labhsetwar, S. Hishita, N. Ohashi, Visible-light-driven photocatalysis on fluorine-doped TiO_2 powders by the creation of surface oxygen vacancies, Chem. Phys. Lett. 401 (2005) 579–584.
[20] D. Li, H. Haneda, S. Hishita, N. Ohashi, Visible-light-driven nitrogen-doped TiO_2 photocatalysts: effect of nitrogen precursors on their photocatalysis for decomposition of gas-phase organic pollutants, Mater. Sci. Eng. B-Solid State Mater. Adv. Technol. 117 (2005) 67–75.
[21] S. Sato, R. Nakamura, S. Abe, Visible-light sensitization of TiO_2 photocatalysts by wet-method N doping, Appl. Catal. A-Gen. 284 (2005) 131–137.
[22] Z. Wang, W. Cai, X. Hong, X. Zhao, F. Xu, C. Cai, Photocatalytic degradation of phenol in aqueous nitrogen-doped TiO_2 suspensions with various light sources, Appl. Catal. B-Environ. 57 (2005) 223–231.
[23] Y.Q. Wang, X.J. Yu, D.Z. Sun, Synthesis, characterization, and photocatalytic activity of $TiO_{2-x}N_x$ nanocatalyst, J. Hazard. Mater. 144 (2007) 328–333.
[24] X. Fang, Z. Zhang, Q. Chen, H. Ji, X. Gao, Dependence of nitrogen doping on TiO_2 precursor annealed under NH_3 flow, J. Solid State Chem. 180 (2007) 1325–1332.
[25] S. Mozia, M. Tomaszewska, B. Kosowska, B. Grzmil, A.W. Morawski, K. Kałucki, Decomposition of nonionic surfactant on a nitrogen-doped photocatalyst under visible-light irradiation, Appl. Catal. B-Environ. 55 (2005) 195–200.
[26] M. Stylidi, D.I. Kondarides, X.E. Verykios, Visible light-induced photocatalytic degradation of acid orange 7 in aqueous TiO_2 suspensions, Appl. Catal. B-Environ. 47 (2004) 189–201.
[27] C. Bauer, P. Jacques, A. Kalt, Photooxidation of an azo dye induced by visible light incident on the surface of TiO_2, J. Photochem. Photobiol. A-Chem. 140 (2001) 87–92.
[28] K. Vinodgopal, D.E. Wynkoop, P.V. Kamat, Environmental photochemistry on semiconductor surfaces: photosensitized degradation of a textile azo dye, acid orange 7, on TiO_2 particles using visible light, Environ. Sci. Technol. 30 (1996) 1660–1666.
[29] B. Muktha, G. Madras, T.N.G. Row, U. Scherf, S. Patil, Conjugated polymers for photocatalysis, J. Phys. Chem. B 111 (2007) 7994–7998.
[30] P. Mahata, G. Madras, S. Natarajan, New photocatalysts based on mixed-metal pyridine dicarboxylates, Catal. Lett. 115 (2007) 27–32.
[31] P. Mahata, G. Madras, S. Natarajan, Novel photocatalysts for the decomposition of organic dyes based on metal-organic framework compounds, J. Phys. Chem. B 110 (2006) 13759–13768.
[32] S. Mahapatra, G. Madras, T.N. Guru Row, Structural and photocatalytic activity of lanthanide (Ce, Pr, and Nd) molybdovanadates, J. Phys. Chem. C 111 (2007) 6505–6511.
[33] M. Sökmen, A. Özkan, Decolourising textile wastewater with modified titania: the effects of inorganic anions on the photocatalysis, J. Photochem. Photobiol. A-Chem. 147 (2002) 77–81.
[34] C. Guillard, H. Lachheb, A. Houas, M. Ksibi, E. Elaloui, J.-M. Herrmann, Influence of chemical structure of dyes, of pH and of inorganic salts on their photocatalytic degradation by TiO_2 comparison of the efficiency of powder and supported TiO_2, J. Photochem. Photobiol. A-Chem. 158 (2003) 27–36.
[35] J. Sun, X. Wang, J. Sun, R. Sun, S. Sun, L. Qiao, Photocatalytic degradation and kinetics of Orange G using nano-sized Sn(IV)/TiO_2/AC photocatalyst, J. Mol. Catal. A-Chem. 260 (2006) 241–246.
[36] J.M. Kwon, Y.H. Kim, B.K. Song, S.H. Yeom, B.S. Kim, J.B. Im, Novel immobilization of titanium dioxide (TiO_2) on the fluidizing carrier and its application to the degradation of azo-dye, J. Hazard. Mater. 134 (2006) 230–236.
[37] G. Sivalingam, K. Nagaveni, M.S. Hegde, G. Madras, Photocatalytic degradation of various dyes by combustion synthesized nano-anatase TiO_2, Appl. Catal. B-Environ. 45 (2003) 23–38.
[38] C. Hachem, F. Bocquillon, O. Zahraa, M. Bouchy, Decolourization of textile industry wastewater by the photocatalytic degradation process, Dyes Pigment. 49 (2001) 117–125.
[39] S. Yang, L. Lou, K. Wang, Y. Chen, Shift of initial mechanism in TiO_2-assisted photocatalytic process, Appl. Catal. A-Gen. 301 (2006) 152–157.
[40] K. Nagaveni, G. Sivalingam, M.S. Hegde, G. Madras, Solar photocatalytic degradation of dyes: high activity of combustion synthesized nano-TiO_2, Appl. Catal. B-Environ. 48 (2004) 83–93.
[41] S.I. Shah, W. Li, C.-P. Huang, O. Jung, C. Ni, Study of Nd^{3+}, Pd^{2+}, Pt^{4+}, and Fe^{3+} dopant effect on photoreactivity of TiO_2 nanoparticles, Proc. Natl. Acad. Sci. U.S.A. 99 (1999) 6482–6486.
[42] N.C. Saha, H.G. Tompkins, Titanium nitride oxidation chemistry: an X-ray photoelectron spectroscopy study, J. Appl. Phys. 72 (1992) 3072–3080.
[43] J.-Q. Wang, W.-H. Wu, D.-M. Feng, Introduction of Electron Spectra (XPS/XAES/UPS), Beijing Industry Press, Beijing, 1992.
[44] R. Marchand, F. Tessier, A. Le Sauze, N. Diot, Typical features of nitrogen in nitride-type compounds, Int. J. Inorg. Mater. 3 (2001) 1143–1146.
[45] N.B. Colthup, L.H. Daly, S.E. Wiberley, Introduction to Infrared and Raman Spectroscopy, second ed., Academic Press, New York, 1975.
[46] X. Zhang, Y. Wang, G. Li, Effect of operating parameters on microwave assisted photocatalytic degradation of azo dye X-3B with grain TiO_2 catalyst, J. Mol. Catal. A-Chem. 237 (2005) 199–205.
[47] M.A. Tariq, M. Faisal, M. Muneer, Semiconductor-mediated photocatalysed degradation of two selected azo dye derivatives, amaranth and bismarck brown in aqueous suspension, J. Hazard. Mater. 127 (2005) 172–179.
[48] M.A. Fox, M.T. Dulay, Heterogeneous photocatalysis, Chem. Rev. 93 (1993) 341–357.
[49] M. Muruganandham, M. Swaminathan, Photocatalytic decolourisation and degradation of reactive orange 4 by TiO_2-UV process, Dyes Pigment. 68 (2006) 133–142.
[50] N. Daneshvar, D. Salari, A.R. Khataee, Photocatalytic degradation of azo dye acid red 14 in water: investigation of the effect of operational parameters, J. Photochem. Photobiol. A-Chem. 157 (2003) 111–116.
[51] N.M. Mahmoodi, M. Arami, N.Y. Limaee, N.S. Tabrizi, Kinetics of heterogeneous photocatalytic degradation of reactive dyes in an immobilized TiO_2 photocatalytic reactor, J. Colloid Interf. Sci. 295 (2006) 159–164.
[52] H.M. Coleman, V. Vimonses, G. Leslie, R. Amal, Degradation of 1.4-dioxane in water using TiO_2 based photocatalytic and H_2O_2/UV processes, J. Hazard. Mater. 146 (2007) 496–501.
[53] K. Tanaka, T. Hisanaga, K. Harada, Efficient photocatalytic degradation of chloral hydrate in aqueous semiconductor suspension, J. Photochem. Photobiol. A-Chem. 48 (1989) 155–159.